Korean J. of Chem. Eng., **13**(5), 515-521 (1996)

MANUFACTURING OF CERAMIC COMPOSITES REINFORCED WITH LAYERED WOVEN FABRICS BY CVI OF SiC FROM DICHLORODIMETHYLSILANE

Min-Soo Cho, Jung-Woo Kim and Gui-Yung Chung†

Department of Chemical Engineering, Hongik University, 72-1 Sangsu-Dong, Mapo-Ku, Seoul 121-791, Korea
(Received 10 May 1996 • accepted 26 August 1996)

Abstract – Manufacturing of ceramic/ceramic composites by chemical vapor infiltration of SiC from dichlorodimethylsilane (DDS) in 2- and 4-ply woven carbon fabrics has been studied. Dense deposition was obtained at a low reaction pressure such as 10 torr, as expected. However, little deposition was occurred at low DDS concentration such as 4%. Spaces between plies were left void with little deposition. The amount of deposition was proportional to the pressure and the DDS concentration. From the experimental data of the amount of deposition, the first order deposition rate constant of 40 cm/min was estimated. This value was bigger than our previous value. The tendencies for 4-ply sample were similar to those of 2-ply sample. Scanning electron microphotographs and pore size distribution analysis showed the same results.

Key words: Layered Woven Fabrics, Chemical Vapor Infiltration, Deposition Rate, Dichlorodimethylsilane, SiC

INTRODUCTION

Ceramic materials have good mechanical properties at high temperature, low density, and resistance to corrosion and erosion. Furthermore, fiber reinforcement adds strength and toughness to ceramic materials. Such fiber-reinforced composites can be prepared by hotpressing and sintering mixtures of powders and chopped fibers and by chemical vapor infiltration (CVI) [Besmann et al., 1991].

CVI was originated in efforts to densify porous graphite bodies by infiltration of carbon. The earliest report of the use of CVI was a patent for infiltrating fibrous alumina with chromium carbides [Jenkin, 1964]. The technique has been developed commercially such that half of the carbon-carbon composites currently produced are made by CVI [Bickerdike et al., 1962]. In CVI, the precursor gas diffuses into a porous ceramic preform, predominantly made up of fiber materials. Then the chemical reaction at pore walls leads to a deposition of matrix materials. Ideally, the result is a dense composite. It can produce large pieces of composite materials with complex shape.

Manufacturing of fiber-reinforced ceramic composites by CVI was studied by many researchers. Ceramic composites reinforced with a fiber bundle were studied by Rossignol et al. [1984] and Tai and Chou [1989]. Those reinforced with short fiber preforms were studied by Gupte and Tsamopoulos [1980], Starr [1987], Jensen and Melkote [1989].

Mathematical modelling of manufacturing of ceramic composites reinforced with multilayer woven fabrics was studied by Chung et al. [1991, 1992, 1993]. An overall deposition reaction which is first order in reactant concentration and in surface area available for deposition was assumed [Chung et al., 1993]. In the previous works [Chung et al., 1991, 1992, 1993], mathematical modelling was confined to the preform itself. In other words, the concentration of the reactant gas outside of the sample was uniform. However, in this research, the whole reactor with a sample inside was the object of modelling. Hence, the concentration outside of the sample was not uniform.

Manufacturing of ceramic SiC/C composites by CVI was studied in this experiment. Deposition in a single ply sample had been carried out by our group [Kim et al., 1996]. Depositions in 2- and 4-ply samples were carried out with the reaction conditions used for the single ply sample. Two void regions in the sample were considered: holes between tows and gaps around filaments in a tow [Chung et al., 1991]. Reactant gases diffuse into the three void regions and react to produce solid deposit. Diffusion of reactant gases from the outside surface into the sample results an internal concentration gradient. This concentration gradient can result in a nonuniform deposition profile in the composite and occlusion of the outer surface of the sample before filling the interior voids completely [Chung et al., 1991].

The objective of this work is to fabricate fiber reinforced SiC/C composites by CVI of SiC from dichlorodimethylsilane (DDS) and H_2. How deposition can be controlled by changing the DDS concentration and the reaction pressure for a uniform deposition in the sample will be studied. With scanning electron microphotographs and the poresize analysis, aspects of deposit were confirmed. Experimental data of the amount of deposition were fitted with results from the mathematical modelling. In the fitting process, the overall 1st-order deposition rate constant was obtained and compared with our previous value [Chung et al., 1992].

MODEL DEVELOPMENT

A mathematical model for the deposition process has already been developed to understand the relationship between the chemical reaction rate and various mass transport mechanisms [Chung et al., 1992, 1993; Kim et al., 1996]. The model pre-

†To whom all correspondences should be addressed.

dicts how concentration, amount of deposition, porosity, and dimensions of the sample change with time. Details of modelling are presented in our previous paper [Kim et al., 1996].

As mentioned earlier, the whole reactor was considered for the mathematical modelling. The simplified homogeneous model [Chung et al., 1992] was used in this research. So spaces between plies was considered as void volume of gaps around filaments.

The following assumptions are used for the modelling. As shown in Fig. 2, I-, II-, IV-regions represent the regions before, above, and after the sample. III-region represents inside of the sample. The length of I- and IV-region is 5 cm, respectively, and the length of sample (II- and III-region) is 3 cm. The substrate consists of fabrics, gaps, and holes and has a porous flat surface with square holes. Filaments within a tow are arranged on triangular centers. There is no concentration gradient in the x-direction. The concentration in the whole system approaches a steady state rapidly. Then, as deposition goes on, the concentration profile changes with the change of porosity and surface area.

The plies are spaced so that holes in every ply are aligned above each other. Diffusion of gaseous DDS occurs from both surfaces to the center of the sample; through the holes and through the gaps around filaments. The model was developed by solving mass balance equations for DDS.

Mass balance equations outside of the sample (II-region) are as follows:

$$\frac{\partial N_{Agx}}{\partial x}+\frac{\partial J_{Agz}}{\partial z}-\frac{2kC_{Ag}}{W}=0 \tag{1}$$

b.c. at z=0, $C_{Ag}|_{z=0}=C_{As}|_{z'=0}$ (before plugging gaps) (2)

$$\frac{\partial N_{Agx}}{\partial x}-\frac{J_{Agz}}{\Delta z}-\left(\frac{2}{W}+\frac{1}{\Delta z}\right)kC_{Ag}=0 \text{ (after plugging gaps)} \tag{3}$$

$$\text{at } z=B,\ -\frac{\partial N_{Agx}}{\partial x}+\frac{J_{Agz}}{\Delta z}-\left(\frac{2}{W}+\frac{1}{\Delta z}\right)kC_{Ag}=0 \tag{4}$$

Eqs. (2) and (3) are the boundary conditions before and after plugging gaps around the outer filaments of the sample. In front of the sample (I-region) and behind the sample (IV-region), depositions occur on the walls of the carbon cylinder. Then a symmetric boundary condition was used instead of Eqs. (2) and (3).

Mass balance equations in the gaps around filaments inside of the sample (III-region) are as follows:

$$\frac{\partial J_{Asz'}}{\partial z'}+F2\pi rkC_{As}=0 \tag{5}$$

b.c. at z'=0, $C_{Ag}|_{z=0}=C_{As}|_{z'=0}$ (6)

$$\text{at } z'=b,\ \frac{\partial C_{Agz'}}{\partial z'}=0 \tag{7}$$

Mass balance equations in the hole before and after plugging hole walls were also developed in the similar way.

The rate of change of the radius of a filament is as follows:

$$\frac{\partial r}{\partial t}=\frac{qM_m k}{\rho_m}C_{As} \tag{8}$$

i.c. $r=r_0$ at $t=0$ (9)

The rate of change of the thickness of the sample is as follows:

$$\frac{\partial b}{\partial t}=-2\frac{qM_m k}{\rho_m}C_{Ag}|_{z=0} \tag{10}$$

i.c. $b=b_0$ at $t\le t_c$ (11)

t_c is plugging time around the filaments of surface.

The rate of change of the thickness of the tube wall is as follows:

$$\frac{\partial B}{\partial t}=-2\frac{qM_m k}{\rho_m}C_{Ag}|_{z=B} \tag{12}$$

i.c. $B=B_0$ at $t=0$ (13)

The amount of deposition could be calculated with changes in dimensions of the sample [Chung et al., 1993; Kim, 1996].

EXPERIMENTAL

The deposition system is shown in Fig. 1. The system consisted of three parts such as a feed supply system, an electric furnace, and a gas draining system. The feed supply system consisted of H_2 and Ar gas cylinders, flow meters, and a DDS vessel. A carbon tube was located in the middle of quartz jacket in the furnace. The gas draining system consisted of a pressure gauge, NaOH trap, and a vacuum pump. The NaOH trap removes HCl in the exit gas. The reagent used was 99% DDS (Jansen Co.).

The multilayer woven fabric sample (Toray, T300 B6000) contained tows of 6000 filaments. Each carbon fiber filament was circular in cross-section and 8 μm in diameter. Each ply of the sample was preprocessed to be an aligned holes. The sample was set in this geometry by coating it with a dilute solution of polymethylmethacrylate. Then, the sample in the sample holder was located in the middle of the carbon tube.

After the system was evacuated, argon gas was flushed to remove air left in the system. After the furnace was heated to the reaction temperature, DDS and H_2 gas entered into the system. Reaction conditions are summarized in Table 1.

The amount of deposition was measured by weighing a sam-

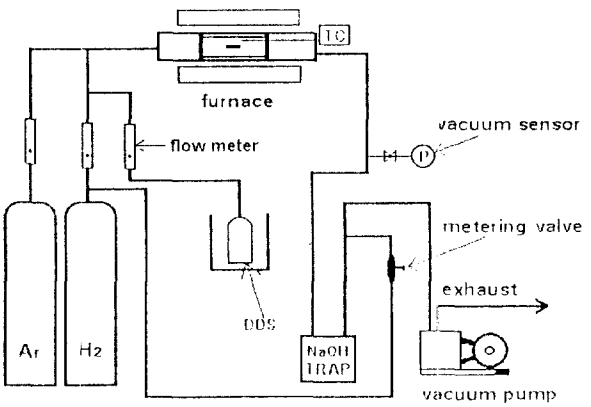

Fig. 1. Schematic diagram of the experimental apparatus.

Table 1. Reaction conditions used in the experiment

Temperature	950°C
Pressure	10, 30 torr
Diffusion coefficient	236 cm^2/min
Flow rate of the carrier gas at 25°C	
11% of DDS	900 cm^3/min
4% of DDS	500 cm^3/min
Number of filaments in a two	12000
Radius of filaments	0.0004 cm
Sample size (2b × L × W)	0.0433 × 2.4 × 3 cm

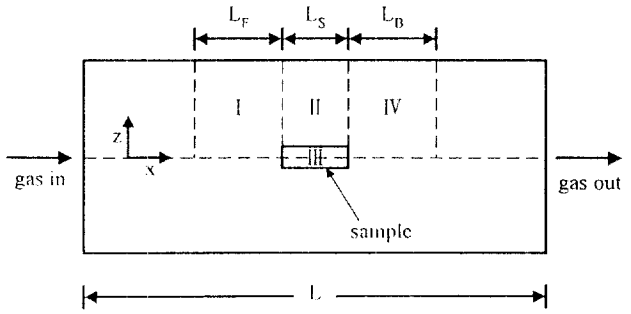

[side view of the reactor]

Fig. 2. Schematic diagram of the system for the numerical analysis.

ple during the deposition reaction. Scanning electron microscopy (Hitachi model S-2500C) and poresizer (Micromeritics model 9320) were used.

RESULTS AND DISCUSSION

1. Deposition Rate

From the mathematical modelling, changes of dimensionless concentration of DDS with dimensionless distance along the axis of tube in the gas phase at the plugging time of the gaps around the outer filaments of the 2-ply sample are shown in Fig. 3. The lines indicate the DDS concentration in I-, II-, IV-regions of Fig. 2. In every region, there is a big concentration decrease following the z-direction. However, the relative reduction of concentration following the z-direction in II-region was more extreme than those in I- and IV-regions due to the large deposition area around filaments. Fig. 3 also shows the concentration decreases following the z'-direction inside of the sample. Line II-1 is the concentration distribution along the graphite tube wall and line II-9 is that on the outside surface of the sample.

The amounts of deposition at different pressures are shown in Fig. 4. The amount of deposition is proportional to the pressure. The plots are linear with one break point as expected. The first slope is due to the deposition in the gaps around filaments. The second one is due to deposition in the spaces between plies and on the surface of the sample. Because of the large surface area on the surface of filaments, the initial slope is much bigger than the second slope. In the actual experiment, the mass of the sample decreased about 30% at the beginning. This is due to firing of epoxy coated on the surface of filaments and vaporizing moisture among filaments. Hence, the

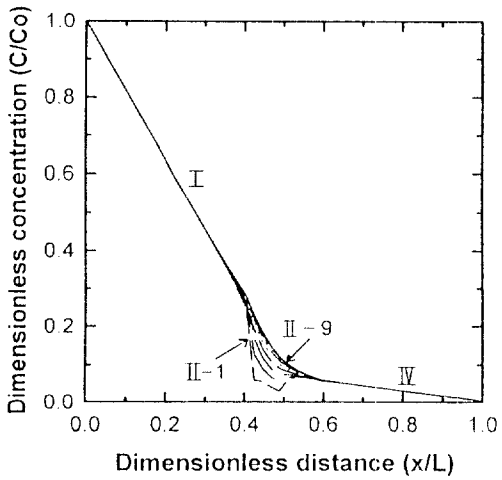

Fig. 3. Changes of dimensionless concentration of DDS with dimensionless distance along the axis of tube at the plugging time of gaps around the outer filaments of the 2-ply sample. Reaction conditions; 950°C, 10 torr, 11% DDS, 900 ml/min.

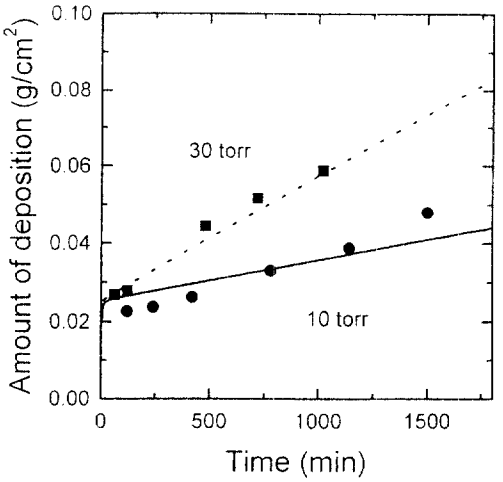

Fig. 4. Changes of the amount of deposition with time at different pressures for the 2-ply sample. Reaction conditions: 950°C, 11% DDS, 900 ml/min. Lines are mathematical modelling results.

first data points in Figs. 4, 6 were adjusted by considering that.

The first-order deposition rate constant of 40 cm/min was estimated by fitting the experimental data with results from the mathematical modelling. This value is bigger than the previous value of 10 cm/min [Chung et al., 1991]. This is because of the difference in the assumed concentration outside of the sample. In this research, there was a concentration gradient outside of the sample along the direction of gas flow. However, in the previous research, the concentration was assumed constant around the sample. The high concentration in the previous research resulted in the smaller value of reaction rate constant.

The amounts of deposition at different concentrations of DDS are shown in Fig. 5. With 40 cm/min of 1st-order deposition rate constant, mathematical modelling results fitted the experimental data well. However, the experimental data of 4%

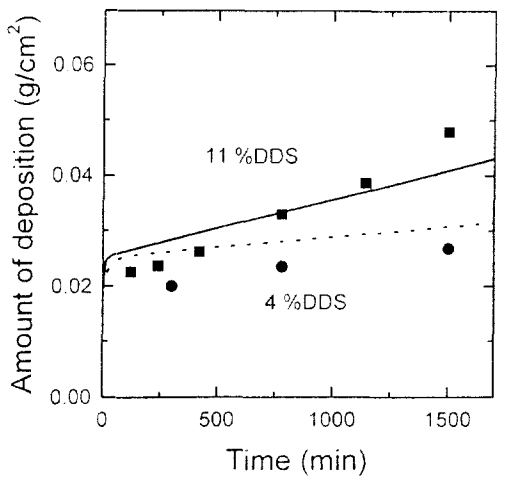

Fig. 5. Changes of the amount of deposition with time at different concentrations for the 2-ply sample. Reaction conditions: 950°C, 10 torr, 900 ml/min for 11% DDS and 500 ml/min for 4% DDS. Lines are mathematical modelling results.

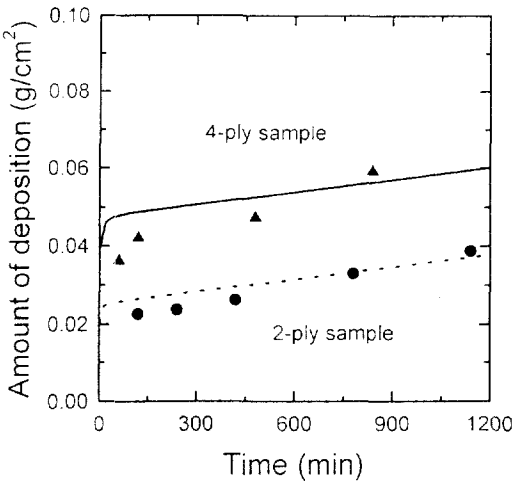

Fig. 6. Changes of the amount of deposition with time for the 2 and 4-ply sample. Reaction conditions; 950°C, 10 torr, 11% DDS, 900 ml/min. Lines are mathematical modelling results.

DDS were a little bit deviated from the modelling line. This is because of the formation of needle-shape deposit. The decrease of partial pressure of DDS due to the resistance of diffusion into the sample became a condition for needle-shape deposit formation. Hence, dense deposition inside the sample was not possible and the amount of deposition was less than the mathematical modelling line with 40 cm/min. However, the trend of the line of the amount of deposition on the surface of the sample for 4% DDS concentration was similar to that for 11% DDS concentration. The amount of deposition for 4-ply sample increased in the similar way to that for 2-ply sample as shown in Fig. 6.

2. Pore Size Distribution

Incremental pore volumes of the 2-ply samples deposited at different pressures and different concentrations of DDS are

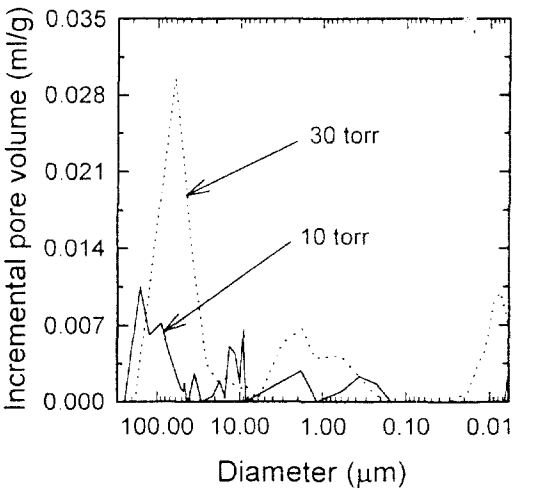

Fig. 7. Changes of the incremental pore volume with diameter at different pressures for the 2-ply sample. Reaction conditions; 950°C, 11% DDS, 900 ml/min.

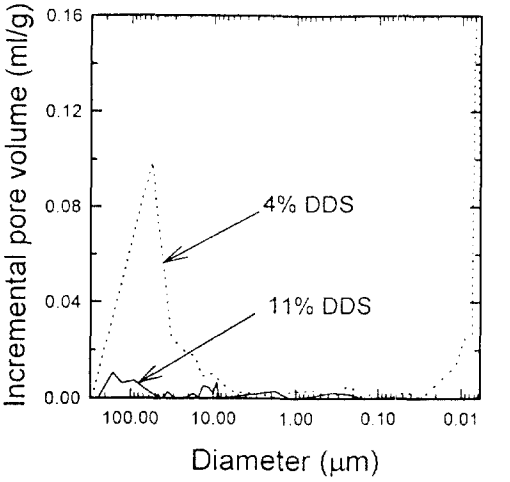

Fig. 8. Changes of the incremental pore volume with diameter at different DDS concentrations for the 2-ply sample. Reaction conditions; 950°C, 10 torr, reaction time, 24 hr for 11% DDS and 54 hr for 4% DDS.

shown in Figs. 7 and 8, respectively. The sample deposited at a high pressure, 30 torr, left more void volume than the sample deposited at a low pressure, 10 torr, did. The peaks of pore diameter around 100 μm and 8 μm indicate spaces between plies, and gaps around filaments. Hence, at 30 torr, gaps around the outer filaments of the sample were plugged, before gaps around the inner side filaments were plugged. As shown in Fig. 7, there are more pore volume in the sample deposited at a high pressure. This certifies again that deposition should be done at a low pressure for more dense deposition. The explanation that the sample deposited at 30 torr shows more deposition in the gaps around the outer filaments and on the flat surface of the sample will be continued the following SEM photo in Fig. 10(c)

In Fig. 8, the sample deposited at a low DDS concentration, 4%, has a more pore volume for all sizes of the pores. This contradicts to our expectation that the more dense deposition is

obtained at a low reactant concentration. It seems that the formation of needle-shape deposit is the main reason of having a more pore volume inside of the sample from the SEM photos in Fig. 13.

The incremental pore volumes for 2- and 4-ply sample are shown in Fig. 9. All sizes of pores for 4-ply samples were left void compared with those for 2-ply samples. For the 4-ply sample, it became hard for the reactant gas to diffuse into the gaps around the inner filaments of the sample. Hence, the 4-ply sample became more spacious after deposition.

3. SEM Observation

The aspects of deposit were also confirmed with scanning electron microphotographs. Photos of the deposited surface of the woven sample are shown in Fig. 10. The photo in Fig. 10(a) is the surface of the sample deposited at a lower pressure and a lower concentration. Compared with the photos in Fig. 10(b) and (c), there are less deposit even if it deposited for the longest time, 54 hr. It is consistent with the results from Figs. 5 and 8 that little deposition was occurred due to the formation

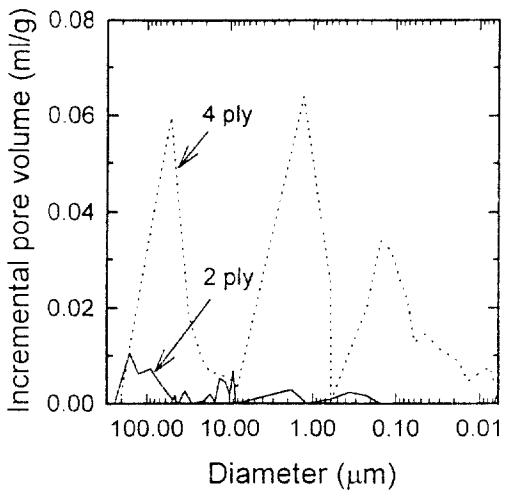

Fig. 9. Changes of incremental pore volume with diameter for 2- and 4-ply samples. Reaction conditions; 950°C, 10 torr, 11% DDS, 900 ml/min, reaction time, 24 hr.

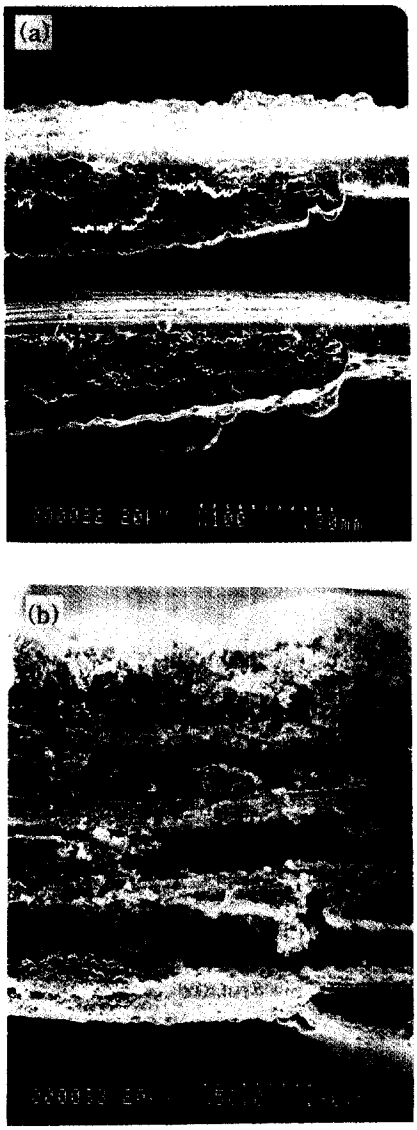

Fig. 11. SEM's of the cross-section of 2- and 4-ply samples. Reaction conditions; 950°C, 10 torr, 11% DDS, 900 ml/min, reaction time 24 hr.

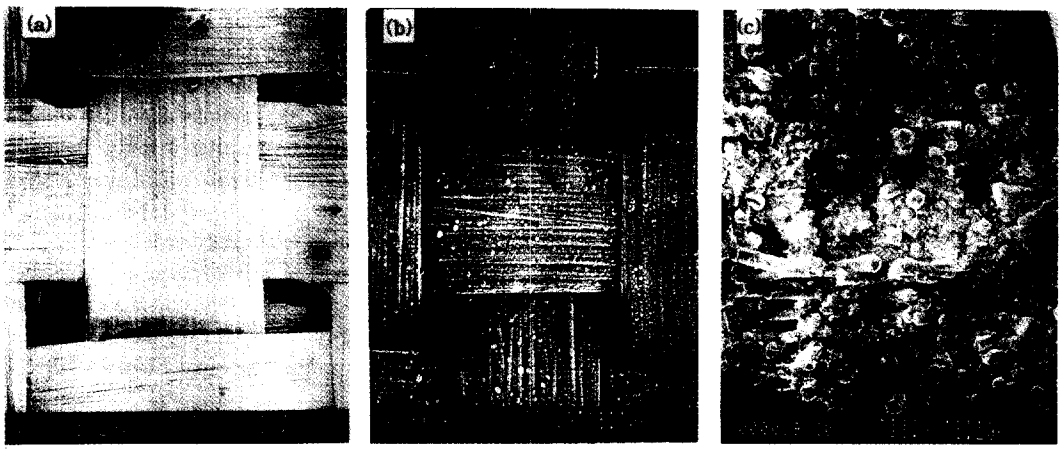

Fig. 10. SEM's of the surface of 2-ply samples deposited at 950°C.
(a) 10 torr, 54 hr, 4% DDS, (b) 10 torr, 24 hr, 11% DDS, (c) 30 torr, 17 hr, 11% DDS.

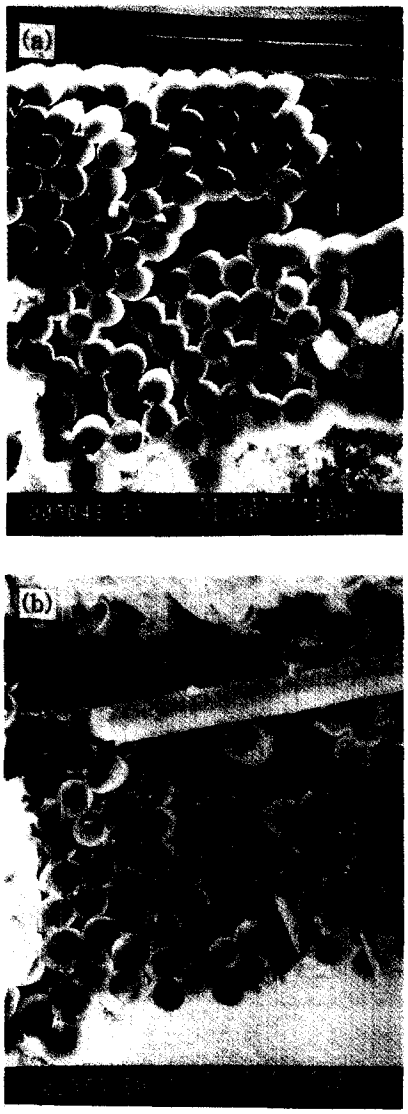

Fig. 12. SEM's of the cross-section of the 4-ply sample. Reaction conditions; 950°C, 10 torr, 11% DDS, 900 ml/min, reaction time 24 hr.
(a) The first ply, (b) The second ply.

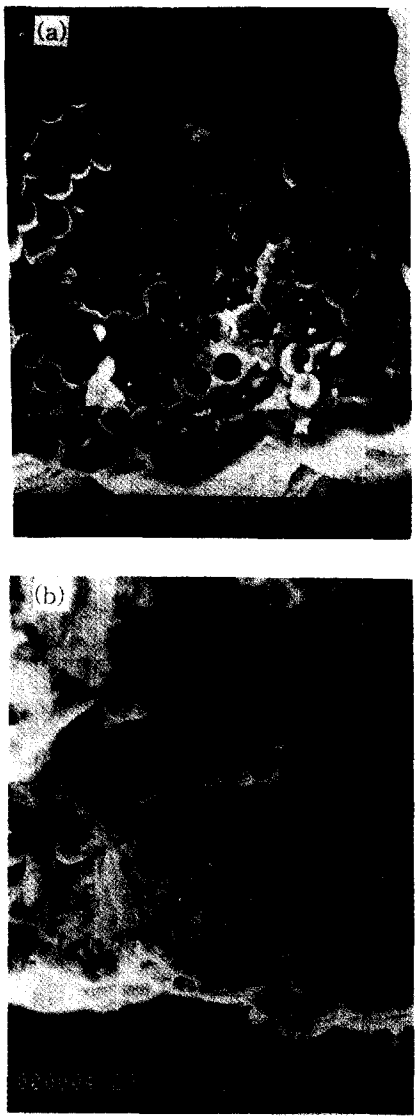

Fig. 13. SEM's of the cross-section of 2-ply samples deposited at 950°C and 10 torr.
(a) 11%, 24 hr, (b) 4%, 110 hr.

of needle-shape deposit. The deposit done at the conditions of 10 torr and 11% DDS in Fig. 10(b) has a small droplet-like deposition sparsely. The surface of the sample deposited at a high concentration and a high pressure in Fig. 10(c) shows a lot of deposit of irregular shape.

Photos of the cross-section of 2- and 4-ply samples are shown in Fig. 11. Surfaces of each ply of the sample are covered with dense deposit. However, spaces between plies are left void. Before the complete plugging of the spaces between plies and the gaps around filaments in the inner plies, the outside surfaces of the outer plies were plugged. So gaps around the outer filaments of the first and the fourth plies in Fig. 11(b) were deposited more than those of the inner plies. Figs. 12(a) and (b) show the different aspects of deposit in the outer ply and the inner ply of the sample. Deposit in the first ply (i.e. the outer ply) is denser than that in the second ply (i.e. the inner ply), as expected.

Photos in Fig. 13 are the cross sections of 2-ply samples deposited with 11% and 4% DDS. Gaps around the outer filaments are plugged before gaps around the inner filaments are filled. Furthermore, the sample deposited with 4% DDS has a lot of pore volume even after a longer reaction time, 110 hr. That is because of the formation of needle-shape deposit. The results are consistent with the results from Figs. 5 and 8. Though, deposition had been carried out for a longer time (i.e. 110 hr), there was a little deposition inside the sample by the reason of the formation of needle-shape deposit. However, for both cases, shapes of deposit on the flat surface of the sample and in the gaps around the outer filaments were similar.

CONCLUSIONS

The chemical vapor infiltration of SiC in 2- and 4-ply woven

fabric samples was studied experimentally in isothermal reactor with a gaseous mixture of reactant DDS and hydrogen. More dense deposition was obtained at a low pressure. For the 4-ply sample, there was a little deposition in the inner plies while gaps of the outer plies were completely plugged. At a low DDS concentration, SiC was deposited a little in the gaps around filaments, even though it was deposited for the longest reaction time. This is because of the formation of needle-shape deposit inside the sample. This was certified with SEM photos and porosity measurements. The rate of deposition was determined from the change of the amount of deposition. The estimated first order rate constant was 40 cm/min, based on the surface area of the sample. The concentration gradient around the sample caused the 1st-order deposition rate constant to be higher than the previous value.

ACKNOWLEDGEMENT

Authors are grateful for the financial support from the Korea Research Foundation, Grant 95-01-E-1011.

NOMENCLATURE

a : side length of the square hole [cm]
B : distance between the inside wall of the tube and the surface of the sample [cm]
b : half of the thickness of the sample [cm]
C_A : mole concentration of the component A [mol/cm^3]
F : number of filaments per unit cross sectional area of a tow [cm^{-2}]
J_A : diffusion flux of the component A [mole/cm^2 sec]
k : first-order deposition rate constant [cm/min]
L : length of the graphite tube [cm]
L_F : length of I-region (in front of the sample) [cm]
L_S : length of II-, III-region (sample) [cm]
L_B : length of IV-region (behind the sample) [cm]
M_m : molecular weight of deposited SiC [g/mol]
N_A : molar flux of the component A [mole/cm^2 sec]
q : number of molecule of Si/SiC generated from a DDS molecule
r : radius of a filament [cm]
t : time [min]
W : width of the graphite tube [cm]
x : coordinate in the direction of diffusion in the space between plies [cm]
z : coordinate in the direction of diffusion above the sample [cm]
z′ : coordinate in the direction of diffusion in the sample [cm]

Greek Letter

ρ_m : density of the deposited material [g/cm^3]

Subscripts

c : plugging time
g : gas phase
o : zero time
s : solid phase
x : x-direction
z, z′ : z- and z′-direction

REFERENCES

Besmann, T. M., Sheldon, B. W., Lowden, R. A. and Stinton, D. P., "Vapor-Phase Fabrication and Properties of Continuous-Filament Ceramic Composites", *Science,* **253**, 1104 (1991).

Bickerdike, R. J., Brown, A. R. G., Hughes, G. and Ranson, H., in Proceedings of the Fifth Conference on Carbon, Pergamon, New York, Vol. 1 (1962).

Chung, G. Y., McCoy, B. J. and Smith, J. M., "Chemical Vapor Infiltration: Modelling Solid Matrix Deposition in Ceramic-ceramic Composites", *Chem. Eng. Sci.,* **46**(3), 723 (1991).

Chung, G. Y., McCoy, B. J., Smith, J. M. and Cagliostro, D. E., "Rate of Chemical Vapor Deposition of Silicon Carbide and Silicon on Single-Layer Woven Fabrics", *J. Am. Ceram. Soc.,* **74**(12), 4473 (1991).

Chung, G. Y., McCoy, B. J., Smith, J. M. and Cagliostro, D. E., "Chemical Vapor Infiltration: Modelling Solid Matrix Deposition for Ceramic Composites Reinforced with Layered Woven Fabrics", *Chem. Eng. Sci.,* **47**(2), 311 (1992).

Chung, G. Y., McCoy, B. J., Smith, J. M. and Cagliostro, D. E., "Chemical Vapor Infiltration: Dispersed and Graded Depositions for Ceramic Composites", *AIChE J.,* **39**(11), 1834 (1993).

Lee, G., McCoy, B. J., Smith, J. M. and Cagliostro, D. E., "Graded Deposition by Chemical Vapor Infiltration of Woven Fabrics", *AIChE J.,* **41**(4), 1037 (1995).

Gupte, S. M. and Tsamopoulos, J. A., "Densification of Porous Material by Chemical Vapor Infiltration", *J. Electrochem. Soc.,* **136**(2), 555 (1989).

Jensen, K. F. and Melkote, R. R., "Chemical Vapor Infiltration of Short Fiber Preforms", Extended Abstracted AIChE Annual Meeting, San Francisco, p. 54 (1989).

Jenkin, W. C., U. S. Patent 3,160, 517 (8 December 1964).

Kim, C. W., Cho, M. S. and Chung, G. Y., "Manufacturing of Ceramic Composites Reinforced with Carbon Fibers through CVI", *HWAHAK KONGHAK,* **34**(4), 443 (1996).

Rossignol, J. Y., Langlais, F., Naslain, R., "A Tentative Modelization of Titanium Carbide C.V.I. within the Pore Network of Two Dimensional Carbon-Carbon Composite Preforms", *Proc. Electrochem. Soc.,* **84**(6), 596 (1984).

Starr, T., "Model for CVI of Short Fiber Preforms", *Ceram. Eng. Sci. Proc.,* **8**(7), 951 (1987).

Tai, N. H. and Chou, T. W., "Analytical Modeling of Chemical Vapor Infiltration of Ceramic Composites", *J. Amer. Ceramic. Soc.,* **72**(3), 414 (1989).